

# Performance bound for localization of a near field source

Vlad M. Chiriac\*, Alexander M. Haimovich\*, Stuart C. Schwartz<sup>†</sup>, and Jason A. Dabin<sup>‡</sup>

\*ECE Dept., CWCSR Lab., New Jersey Institute of Technology, Newark, New Jersey

<sup>†</sup>EE Dept, Princeton University, Princeton, New Jersey

<sup>‡</sup>U.S. Army Communications-Electronics Research, Development and Engineering Center  
Fort Monmouth, New Jersey

**Abstract**—The Ziv-Zakai bound (ZZB) is developed for the estimation error of a radiating source located in a plane, and observed by sensors widely distributed over the same plane. The source is non-cooperative in the sense that the transmitted waveform and its timing are unknown to the sensors. The sensors do have however, information on the power spectral density of the source. Moreover, sensors have ideal mutual time and phase synchronization. The source location is estimated by coherent processing exploiting the amplitude and phase information between pairs of sensors. An analytical expression is developed for the ZZB relating the estimation error to the carrier frequency, signal bandwidth, the number of sensors, and their location. Numerical examples demonstrate that the ZZB closely predicts the performance of the maximum likelihood estimate across the full range of signal to noise ratio (SNR) values. At low SNR, the ZZB bound demonstrates performance dominated by noise, at medium SNR, the performance is dictated by the presence of sidelobes in the localization metric, and at high SNR, it is shown that the ZZB converges to the Cramer-Rao bound.

**Index Terms**—Source Localization, Performance Bounds, Parameter Estimation

## I. INTRODUCTION

Source localization has been studied intensively and applied broadly in various fields including radar, sonar, seismic analysis, and sensor networks. Due to the new requirements and technology advances, the localization problem remains an active subject of research. Of interest in this work is the passive localization of non-cooperative sources, i.e., sources for which the actual signal and the time and phase of the transmitted signal are unknown to the sensors. A class of localization techniques for this case is based on time difference of arrival (TDOA). TDOA based localization can be accomplished either by formulating a joint statistic that incorporates all TDOA observations or by performing ranging between pairs of sensors and subsequently, solving a set of nonlinear equations to estimate the source location. TDOA based localization is non-coherent in the sense that it exploits the envelope, but not the phase, of signals observed at the sensors. Recent work on localization employing active sensors (i.e., sensor that transmit probing signals, such as in radar) has shown the potential for significant gains when the localization processing exploits the phase information among pairs of sensors [1]. We refer to such techniques as *coherent* localization. Coherent techniques

have been shown to offer great improvements in accuracy, particularly at high signal to noise ratio (SNR) [1]. This is due to the fact that the accuracy in coherent localization, as expressed through the Cramer-Rao bound, is proportional to the carrier frequency of the observed signal, whereas for non-coherent localization, the accuracy is proportional to the bandwidth of the observed signal. Accuracy also improves with the increase in the number of sensors and the angular sector of their spread (relative to the source). However, large separation between sensors yields, for a fixed number of sensors, high peak sidelobes in the coherent localization metric [2]. At sufficiently high SNR, these sidelobes have only limited impact on performance. However, below a threshold SNR value, performance degrades very quickly. The main goal of the present work is to improve the understanding and develop ways to predict the performance of localization techniques as a function of SNR and also system parameters. Localization performance can be studied through a lower bound on the mean square error (MSE) of the localization estimates. For high SNR, the estimated parameter is affected by small noise errors that cannot cast the estimate outside the main lobe of the estimation metric. In this region, the mean square error (MSE) of the estimate is inversely proportional to the Fisher information, and thus performance can be predicted by calculating the Cramer-Rao lower bound (CRLB), [3]. At low SNR, due to the effect of sidelobes, performance is affected by large errors, and the CRLB cannot predict performance anymore. In this region, performance can be lower bounded by the Ziv-Zakai Bound (ZZB), [4].

In the literature, the ZZB was used as a lower bound for different estimators related to the localization problem. Weiss and Weinstein derived the ZZB for time delay estimation of narrowband [5] and wideband [6] signals. Extending this work, the ZZB for time delay estimation of ultra-wideband signals was studied in [7]. Bell et al. extended the ZZB from scalar to vector parameter estimation [8], and used it to develop a lower bound on the MSE in estimating the 2-D bearing of a narrowband plane wave [9].

The work presented in this paper derives the ZZB for the localization problem of a source. The results obtained in the sequel can be applied to study the performance of the location estimator as a function of different parameters e.g., carrier frequency, bandwidth of the transmitted signal, and the number of sensors in the network. Comparison between the ZZB and

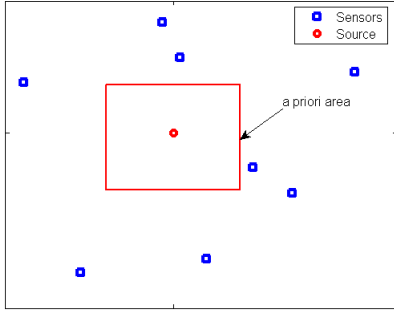


Figure 1. The setup for the localization problem

the MSE of the maximum likelihood estimate (MLE) obtained through simulations demonstrate that the bound is tight in all SNR regions.

The paper is organized as follows. Section II introduces the system model; the derivation of the ZZB is carried out in Section III. Numerical examples are presented in Section IV, and concluding remarks are found in Section V.

## II. SYSTEM MODEL

Consider a radiating source located at an unknown position  $\theta = [x_e, y_e]$ , where  $\theta$  is modeled as a continuous random variable with a known *a priori* probability density function (pdf), assumed here to be the uniform distribution  $x_e, y_e \sim U[-D, D]$ . This description implies that the source is known to be located somewhere in a square area of dimensions  $2D \times 2D$ . The signal emitted by the source has bandwidth  $B$ , and it modulates a carrier frequency  $f_c$ . The source is not cooperating with the sensors, in the sense that the timing of the transmission and the transmitted signal are unknown to the sensors. It is assumed, however, that the sensors are synchronized in both time and phase. We refer to the localization method employed in this paper as *coherent*. With coherent localization, the source location is estimated from amplitude and phase measurements at the sensors. This approach is similar to measurements of signals received across a phased array for bearing estimation. In the bearing estimation problem, the source is in the far-field of the array. In the source localization problem, the source is in the near-field of the two-dimensional array formed by the sensors. In the near field, the phase and amplitude received at each sensor depend on the source location (i.e., range and bearing), not only on the bearing, as in the far field case. Coherent source localization is a passive variation of the recent work on coherent localization with active sensors (i.e., radar), e.g., [1]. Since the transmission time is unknown, coherent localization of the source is performed using phase measurements relative to one of the sensors chosen as the reference sensor.

Source observations are collected by  $M$  sensors located at arbitrary coordinates  $(x_k, y_k)$ ,  $k = 1, \dots, M$ . The period of time  $T$  during which these observations are collected is such that  $BT \gg 1$ . A figure showing the setup is presented in Fig. 1.

Localization of the source is based on noisy observations of the signals received at the sensors and expressed as:

$$r_k(t) = a_k s(t - \tau_k) e^{-j2\pi f_c \tau_k} + w_k(t), \quad k = 1, 2, \dots, M, \quad 0 \leq t \leq T, \quad (1)$$

where  $s$  and  $w_k$  denote respectively, the transmitted signal, and additive noise at the  $k$ -th sensor. The source and the noise waveforms are sample functions of uncorrelated, zero-mean, stationary Gaussian random processes with spectral densities  $P_s$  and  $P_w$ , respectively. The spectral densities are constant across the bandwidth. The amplitude and the propagation delay of the signal received at sensor  $k$  relative to the reference sensor are denoted  $a_k$  and  $\tau_k$ , respectively. Without loss of generality, the reference sensor is indexed 1. The TDOA corresponding to sensor  $k$  is related to the source and  $k$ th sensor coordinates by:

$$\tau_k = \frac{\sqrt{(x_e - x_k)^2 + (y_e - y_k)^2}}{c} - \frac{\sqrt{(x_e - x_1)^2 + (y_e - y_1)^2}}{c}, \quad (2)$$

where  $c$  is the signal propagation speed.

To make use of properties of the Fourier transform, we convert the time domain measurements to the frequency domain. The  $f_l$  Fourier coefficient of the observed signal at sensor  $k$  is given by:

$$\begin{aligned} R_k(f_l) &= \frac{1}{\sqrt{T}} \int_0^T r_k(t) e^{-j2\pi f_l t} dt \\ &= a_k S(f_l) e^{-j2\pi(f_l + f_c)\tau_k} + W_k(f_l), \quad k = 1, 2, \dots, M, \end{aligned} \quad (3)$$

where  $l = 1, \dots, N$ ,  $N$  is the number of frequency samples, and  $S(f_l)$  and  $W_k(f_l)$  are the Fourier coefficients at  $f_l$  of  $s(t)$  and  $w_k(t)$ , respectively. For later use, we define the vectors  $\mathbf{r} = [\mathbf{r}(f_1), \mathbf{r}(f_2), \dots, \mathbf{r}(f_N)]^T$ , where  $\mathbf{r}(f_l) = [R_1(f_l), R_2(f_l), \dots, R_M(f_l)]^T$ . For  $BT \gg 1$ , any pair of Fourier coefficients is uncorrelated [10]. Since  $r_k(t)$  is a Gaussian process and the Fourier transform is a linear operation,  $\mathbf{r}$  has a conditional multivariate Gaussian pdf,

$$\begin{aligned} p(\mathbf{r}|\theta) &= \prod_{l=1}^N \det[\pi \mathbf{K}(f_l)]^{-1} \\ &\quad \cdot \exp(-\mathbf{r}^H(f_l) \mathbf{K}^{-1}(f_l) \mathbf{r}(f_l)), \end{aligned} \quad (4)$$

where the covariance matrix of the Fourier coefficients at the sensors is given by

$$\begin{aligned} \mathbf{K}(f_l) &= E[\mathbf{r}(f_l) \mathbf{r}^H(f_l)] \\ &= P_s \gamma(f_l) \gamma^H(f_l) + P_w \mathbf{I}, \end{aligned} \quad (5)$$

In this expression,  $P_s$  and  $P_w$  were defined previously, and the vector  $\gamma(f_l) = [1, a_2 e^{-j2\pi(f_c + f_l)\tau_2}, \dots, a_M e^{-j2\pi(f_c + f_l)\tau_M}]^T$  represents the response across the sensors to a radiated frequency component  $(f_c + f_l)$ . The matrix  $\mathbf{I}$  is the identity matrix. The superscripts “ $T$ ” and “ $H$ ” denote the transpose and conjugate transpose operations, respectively.

The maximum likelihood estimate of the source location is given by the maximum of the likelihood function

$$\hat{\theta}_{ML}(\mathbf{r}) = \arg \max_{\theta} p(\mathbf{r}|\theta) \quad (6)$$

where the likelihood function equals the value of the pdf at the observations  $\mathbf{r}$ . It can be shown that for the model defined in (4) and (5), the MLE of  $\theta$  is given by the expression:

$$\hat{\theta}_{ML}(\mathbf{r}) = \arg \max_{\theta} \sum_{l=1}^N |\mathbf{r}^H(f_l)\gamma(f_l)|^2 \quad (7)$$

The former expression reveals the coherent nature of the estimator, since the phases of the elements of the vector  $\gamma(f_l)$  are functions of the location  $\theta$ .

It is well known that a linear phased array in which the elements are highly thinned, has a beampattern with large sidelobes. In particular, when the elements of the array are randomly spaced at intervals of the order of 10's or 100's of wavelengths, the beampattern has random peak sidelobes [11]. Recent work on coherent MIMO radar based in a setting of widely spaced transmitters and receivers also shows the presence of large peak sidelobes [2]. Similar sidelobes are present in the localization metric (7). This motivates our work to develop a global bound on the localization performance, as presented in the next section.

### III. LOCALIZATION ESTIMATION BOUND

Consider the problem of estimating the position vector,  $\theta$ , of the emitting source. We are interested in deriving lower bounds for the mean square error (MSE) of the individual components of  $\theta$ . The lower bounds should predict as nearly as possible the performance of the maximum likelihood estimator (MLE) for the whole SNR region. In the literature, one of the most popular bounds used to predict the performance of the MLE is the Cramer Rao lower bound (CRLB), [12]. The justification of using CRLB resides in that the MLE approaches the CRLB arbitrarily close for very long observations. CRLB is a local bound error performance i.e., it represents the performance of estimators only for small errors. As the SNR decreases, the errors become global and spread beyond the local vicinity of the true value of the estimated parameter. Thus, the CRLB cannot be used to predict the MLE performance under these conditions.

When global errors are of interest, evaluating them is meaningful only if the set of possible values of the parameters to be estimated is known beforehand. This leads to Bayesian type bounds. The characteristic of these bounds is that, they assume a random parameter model with known *a priori* distribution. In the literature, several Bayesian bounds were proposed, [13], [4], [14], [15], [16]. In this work, we focus on the Ziv-Zakai bound (ZZB) [4], [14].

Briefly, in its scalar form, the problem is that of lower bounding the MSE

$$E[\epsilon^2] = E\left[\left|\hat{\theta}(r) - \theta\right|^2\right] \quad (8)$$

where  $\theta$  is the true value and  $\hat{\theta}$  is the estimate. The derivation for the scalar case starts with the MSE computed globally from the identity [8],

$$E[\epsilon^2] = \frac{1}{2} \int_0^\infty \Pr\left(|\epsilon| \geq \frac{h}{2}\right) h dh \quad (9)$$

and focuses on lower bounding  $\Pr(|\epsilon| \geq \frac{h}{2})$ . The estimation probability of error  $\Pr(|\epsilon| \geq \frac{h}{2})$  can be viewed from a detection theory point of view by noting that  $\Pr(|\epsilon| \geq \frac{h}{2})$  is also the probability of a binary hypothesis problem in which  $\theta$  equals either some value  $\varphi$  ( $H_0$  hypothesis) or the value  $\varphi + h$  ( $H_1$  hypothesis).

In the localization problem, the unknown parameter is represented by a vector  $\theta$ . Hence, we are interested in the extension of the ZZB to vector parameters. In particular, the extended ZZB for vector parameter estimation, which was derived in [8], is customized in this section for the problem of estimating the position of a source. For the position vector,  $\theta = [x_e, y_e]^T$ , the error correlation matrix of the estimator  $\hat{\theta}(\mathbf{r})$  is

$$\Phi = E_{\theta, \mathbf{r}}[\epsilon\epsilon^T] = E_{\theta, \mathbf{r}}[(\hat{\theta}(\mathbf{r}) - \theta)(\hat{\theta}(\mathbf{r}) - \theta)^T], \quad (10)$$

where  $\mathbf{r}$  is the vector of Fourier coefficients representing the noisy observations at the sensors defined in (4), and  $E_{\theta, \mathbf{R}}$  is the expectation with respect to the joint pdf of  $\theta$  and  $\mathbf{r}$ . Lower bounding  $\mathbf{u}^T \Phi \mathbf{u}$  for any vector  $\mathbf{u}$  offers a flexible approach through which the total error (sum of the diagonal elements of  $\Phi$ ) or errors of specific components of  $\theta$  can be bounded. For example, for evaluation of the total error, let  $\mathbf{u} = [1, 1]^T$ ; for estimating the error in the  $x$  coordinate,  $\mathbf{u} = [1, 0]^T$ .

An identity similar to (9) can be written for the vector estimation case by replacing  $|\epsilon|$  with  $|\mathbf{u}^T \epsilon|$ ,

$$\mathbf{u}^T \Phi \mathbf{u} = E[|\mathbf{u}^T \epsilon|^2] = \frac{1}{2} \int_0^\infty \Pr\left(|\mathbf{u}^T \epsilon| \geq \frac{h}{2}\right) h dh. \quad (11)$$

As we discussed previously for the scalar case, the lower bound of  $\Pr(|\mathbf{u}^T \epsilon| \geq \frac{h}{2})$  is obtained by linking the estimation of  $\theta$  with a binary hypothesis testing problem. The vector parameter  $\theta$  is equal to either the vector  $\varphi$  or to the vector  $\varphi + \delta$ . The binary decision problem based on a localization estimate  $\hat{\theta}(\mathbf{r})$  is formulated as follows:

$$\begin{aligned} \text{Decide } H_0: \theta = \varphi & \quad \text{if } \mathbf{u}^T \hat{\theta}(\mathbf{r}) \leq \mathbf{u}^T \varphi + \frac{h}{2} \\ \text{Decide } H_1: \theta = \varphi + \delta & \quad \text{if } \mathbf{u}^T \hat{\theta}(\mathbf{r}) \geq \mathbf{u}^T \varphi + \frac{h}{2} \end{aligned} \quad (12)$$

The separation between the two decision regions is provided by the line  $\mathbf{u}^T \varphi + \frac{h}{2}$ . The probability of error for this detection problem can be lower bounded with the help of the minimum probability of error  $P_e(\varphi, \varphi + \delta)$  of a binary detection problem, in which the transmitted vectors are either  $\varphi$  or  $\varphi + \delta$ . Such a minimum probability of error is obtained from the likelihood ratio test.

In [17], it is shown that the extended ZZB for vector parameter estimation in the case of equally likely hypotheses is given by

$$\mathbf{u}^T \Phi \mathbf{u} \geq \int_0^\infty h \cdot V \left\{ \max_{\delta: \mathbf{u}^T \delta = h} \int_{\Theta} \min[p_\theta(\varphi), p_\theta(\varphi + \delta)] \cdot P_e(\varphi, \varphi + \delta) d\varphi \right\} \cdot dh \quad (13)$$

where  $V\{\cdot\}$  is the valley-filling function, and  $\theta \in \Theta$ . To get insight into the role of the valley-filling function, one must note that in general  $\Pr(|\mathbf{u}^T \boldsymbol{\epsilon}| \geq \frac{h}{2})$  is a non-increasing function of  $h$ . Thus, a tighter lower bound of  $\Pr(|\mathbf{u}^T \boldsymbol{\epsilon}| \geq \frac{h}{2})$  can be obtained by capping the computed lower bound with a non-increasing function of  $h$ . This transformation is done by the valley-filling function.

Assuming uniform, *a priori* pdf's in the interval  $[-D, D]$  for the  $x, y$  coordinates of the emitting source, equation (13) can be specialized as follows

$$\mathbf{u}^T \boldsymbol{\Phi} \mathbf{u} \geq \int_0^{2D} \frac{h}{4D^2} \cdot \left\{ \max_{\delta: \mathbf{u}^T \boldsymbol{\delta} = h} \int_{\Theta} P_{\epsilon}(\varphi, \varphi + \delta) d\varphi \right\} dh \quad (14)$$

As can be observed from (14), the main part of the bound is represented by  $P_{\epsilon}(\varphi, \varphi + \delta)$ . A closed form for  $P_{\epsilon}(\varphi, \varphi + \delta)$  doesn't exist, however an approximation of  $P_{\epsilon}$  can be obtained using Chernoff's formula [12, pp 125]:

$$\begin{aligned} P_{\epsilon}(\varphi, \varphi + \delta) &\approx \frac{1}{2} \exp\left(\mu(s_m) + \frac{s_m^2}{2} \ddot{\mu}(s_m)\right) \\ &\cdot Q\left(s_m \sqrt{\ddot{\mu}(s_m)}\right) + \\ &+ \frac{1}{2} \exp\left(\mu(s_m) + \frac{(1-s_m)^2}{2} \ddot{\mu}(s_m)\right) \\ &\cdot Q\left((1-s_m) \sqrt{\ddot{\mu}(s_m)}\right), \end{aligned} \quad (15)$$

where  $\mu(s)$  is the semi-invariant moment generating function,  $\ddot{\mu}(s)$  is the second derivative of  $\mu(s)$  with respect to  $s$ ,  $s_m$  is the point for which  $\dot{\mu}(s_m) = 0$ , and  $Q(z)$  is the Gaussian integral

$$Q(z) = \int_z^{\infty} \frac{1}{\sqrt{2\pi}} e^{-v^2/2} dv$$

The semi-invariant moment generating function  $\mu(s)$  is defined [12, pp 119]

$$\mu(s) = \ln \int p(\mathbf{r}|\varphi + \delta)^s p(\mathbf{r}|\varphi)^{1-s} d\mathbf{R} \quad (16)$$

Substituting the expression for  $p(\mathbf{r}|\theta)$  given in (4) into (16), and using the result from [18, pp 47], the semi-invariant moment generating function can be rewritten as follows

$$\begin{aligned} \mu(s) &= -\frac{1}{2} \sum_{l=1}^N \ln \left( \det[\mathbf{K}(f_l)]^{-s} \det[\mathbf{K}_{\delta}(f_l)]^{-(1-s)} \right. \\ &\cdot \left. \det[s\mathbf{K}(f_l, \tau) + (1-s)\mathbf{K}_{\delta}(f_l)] \right) \end{aligned} \quad (17)$$

where

$$\begin{aligned} \mathbf{K}_{\delta}(f_l) &= P_s \gamma_{\delta}(f_l) \gamma_{\delta}^H(f_l) + P_w \mathbf{I} \\ \gamma_{\delta}(f_l) &= [1, \dots, a_M e^{-j2\pi(f_l + f_c)(\tau_M + d_M)}]^T \\ d_k &= \frac{1}{c} \left( \sqrt{(x_e + \delta_x - x_k)^2 + (y_e + \delta_y - y_k)^2} - \right. \\ &\quad \left. - \sqrt{(x_e + \delta_x - x_1)^2 + (y_e + \delta_y - y_1)^2} \right) - \\ &\quad - \frac{1}{c} \left( \sqrt{(x_e - x_k)^2 + (y_e - y_k)^2} - \right. \\ &\quad \left. - \sqrt{(x_e - x_1)^2 + (y_e - y_1)^2} \right), \quad k = \overline{2, M} \end{aligned} \quad (18)$$

The first two determinants from equation (17) can be easily calculated using the matrix formula given in [19], and they are given by

$$\det[\mathbf{K}(f_l)] = P_w^M \left( 1 + \frac{P_s}{P_w} \beta \right) = \det[\mathbf{K}_{\delta}(f_l)] \quad (19)$$

where

$$\beta = \left( 1 + \sum_{k=2}^M a_k^2 \right) \quad (20)$$

The derivation of the third determinant can be done using the approach in [20]. After some algebra, the following expression is obtained for the third determinant

$$\begin{aligned} \det[s\mathbf{K}(f_l) + (1-s)\mathbf{K}_{\delta}(f_l)] &= \\ &= P_w^M \left( 1 + \frac{P_s}{P_w} \beta + \right. \\ &\quad \left. + s(1-s) \left( \frac{P_s}{P_w} \right)^2 (\beta^2 - g(f_l)) \right) \end{aligned} \quad (21)$$

where

$$g(f_l) = \frac{|\gamma_{\delta}^H(f_l) \gamma(f_l)|^2}{\beta^2}$$

and  $|\cdot|$  denotes the absolute value.

Substitution of (19) and (21) into (17) gives

$$\mu(s) = - \sum_{l=1}^N \ln(1 + s(1-s)\alpha(1-g(f_l))) \quad (22)$$

where

$$\alpha = \frac{\beta^2 \left( \frac{P_s}{P_w} \right)^2}{1 + \beta \left( \frac{P_s}{P_w} \right)}. \quad (23)$$

Differentiating with respect to  $s$  yields

$$\dot{\mu}(s) = - \sum_{l=1}^N \frac{(1-2s)\alpha(1-g(f_l))}{1 + s(1-s)\alpha(1-g(f_l))} \quad (24)$$

$$\begin{aligned} \ddot{\mu}(s) &= \sum_{l=1}^N \left[ \left( \frac{(1-2s)\alpha(1-g(f_l))}{1 + s(1-s)\alpha(1-g(f_l))} \right)^2 + \right. \\ &\quad \left. + \frac{2\alpha(1-g(f_l))}{1 + s(1-s)\alpha(1-g(f_l))} \right]. \end{aligned} \quad (25)$$

Solving the equation  $\dot{\mu}(s) = 0$ , results in  $s = \frac{1}{2}$ . For  $s = \frac{1}{2}$ , equations (22) and (25) reduce to

$$\begin{aligned}
\mu\left(\frac{1}{2}\right) &= -\sum_{l=1}^N \ln\left(1 + \frac{1}{4}\alpha(1-g(f_l))\right) \xrightarrow{BT \gg 1} \\
&\quad -T \int_{-B/2}^{B/2} \ln\left(1 + \frac{1}{4}\alpha(1-g(f))\right) df \\
\ddot{\mu}\left(\frac{1}{2}\right) &= \sum_{l=1}^N \frac{2\alpha(1-g(f_l))}{1 + \frac{1}{4}\alpha(1-g(f_l))} \xrightarrow{BT \gg 1} \\
&\quad T \int_{-B/2}^{B/2} \frac{2\alpha(1-g(f))}{1 + \frac{1}{4}\alpha(1-g(f))} df.
\end{aligned} \tag{26}$$

If we use the notation

$$\xi(f) = \frac{1}{4}\alpha(1-g(f)),$$

$\mu(\frac{1}{2})$  and  $\ddot{\mu}(\frac{1}{2})$  have the following forms

$$\begin{aligned}
\mu\left(\frac{1}{2}\right) &= -T \int_{-B/2}^{B/2} \ln(1 + \xi(f)) df, \\
\ddot{\mu}\left(\frac{1}{2}\right) &= T \int_{-B/2}^{B/2} 8 \frac{\xi(f)}{1 + \xi(f)} df.
\end{aligned} \tag{27}$$

Using (27) and the following inequalities

$$\begin{aligned}
\ln(1+z) - z &\leq \frac{1}{2}z^2, \text{ for } 0 \leq z \leq 1 \\
\frac{z}{1+z} &\leq z, \text{ for } 0 \leq z \leq 1
\end{aligned} \tag{28}$$

in (15),  $P_\epsilon(\varphi, \varphi + \delta)$  is lower bounded by:

$$\begin{aligned}
P_\epsilon(\varphi, \varphi + \delta) &\geq \exp\left(-T \int_F \frac{1}{2}\xi^2(f)df\right) \\
&\quad \cdot Q\left(\sqrt{2T \int_F \xi(f)df}\right)
\end{aligned} \tag{29}$$

It is noted that  $P_\epsilon(\varphi, \varphi + \delta)$  doesn't depend on  $\varphi$ , but only on  $\delta$ .

The final version of the ZZB lower bound for location estimate is:

$$\begin{aligned}
\mathbf{u}^T \Phi \mathbf{u} &\geq \frac{1}{4D^2} \int_0^{2D} h \cdot \left\{ \max_{\delta: \mathbf{u}^T \delta = h} (2D - u_1 \delta_1)(2D - u_2 \delta_2) \right. \\
&\quad \left. \cdot \exp\left(-T \int_F \frac{1}{2}\xi^2(f)df\right) Q\left(\sqrt{2T \int_F \xi(f)df}\right) \right\} dh,
\end{aligned} \tag{30}$$

where

$$\begin{aligned}
\xi(f) &= \frac{1}{4}\alpha \left(1 - \frac{|\gamma_\delta^H(f)\gamma(f)|^2}{\beta^2}\right), \\
\alpha &= \frac{\beta^2 \left(\frac{P_s(f)}{P_w(f)}\right)^2}{1 + \beta \left(\frac{P_s(f)}{P_w(f)}\right)}, \text{ and } \beta = \left(1 + \sum_{k=2}^M a_k^2\right).
\end{aligned}$$

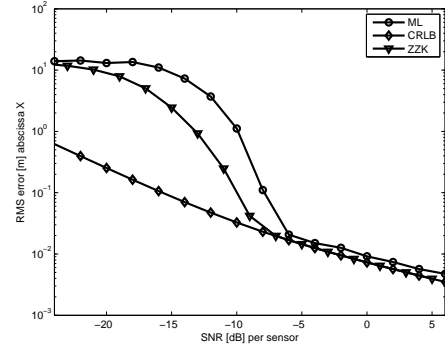


Figure 2.  $M = 8$  sensors, for bandwidth  $B = 200$  kHz, for carrier frequency  $f_c = 100$  MHz, and coordinates  $x_e$  and  $y_e$  uniformly distributed on  $[-25 \text{ m}, 25 \text{ m}]$  with variance  $\sigma_{x_e}^2 = \frac{25^2}{3}$

#### IV. NUMERICAL EXAMPLES

In this section, numerical examples are provided to illustrate the ZZB for various cases of the source localization problem. We present results of the ZZB parameterized by the carrier frequency, bandwidth, and number of sensors. The setup has sensors equally spaced on a circle with a source located at the center of the circle. The duration of the observation was taken to be  $T = 4.3$  milliseconds.

In Fig. 2, the ZZB obtained by numerical integration of (30) is plotted versus the SNR per sensor,  $P_s/P_w$ . The CRLB and the root mean square error (RMSE) of the MLE of the source location are also plotted for reference. The RMSE of the MLE is computed from one thousand simulations of a sequence of raised cosine pulses. The various metrics were calculated for  $M = 8$  sensors, bandwidth  $B = 200$  kHz, and for a carrier frequency  $f_c = 100$  MHz. The *a priori* interval for the coordinates of the source is set to a square with a side equal to 50 m. From the figure it can be observed that the ZZB versus SNR can be divided into three regions. For low SNR, the ZZB reaches a plateau equal to the standard deviation of the *a priori* pdf of the source location, computed as  $\sqrt{\frac{D^2}{3}} = \frac{25}{\sqrt{3}}$ . In this region performance is dominated by noise, hence the localization error is limited only by the *a priori* information. For high SNR, the ZZB coincides with the CRLB, indicating that the noise errors are too small to cast the estimate outside the main lobe of the estimation metric. This region is the ambiguity free region. Between the two SNR extremes is the ambiguity region, in which the location estimator is affected by ambiguities created by sidelobes of the localization metric, [2].

In Fig. 3, the ZZB of the error in estimating the abscissa  $x_e$  of the source is presented for different carrier frequencies. The results presented in the figure were obtained for  $M = 8$  sensors and  $B = 200$  kHz signal bandwidth. The *a priori* interval for the abscissa  $x_e$  of the narrowband source was set to  $[-250 \text{ m}, 250 \text{ m}]$  around the real abscissa. One can observe that if the SNR is high enough, localization accuracy improves with the carrier frequency. The exception is in the ambiguity region where the performance of the estimator at  $f_c = 100$  MHz may outperform the performance at  $f_c = 1$  GHz. This result can be explained due to the increase in

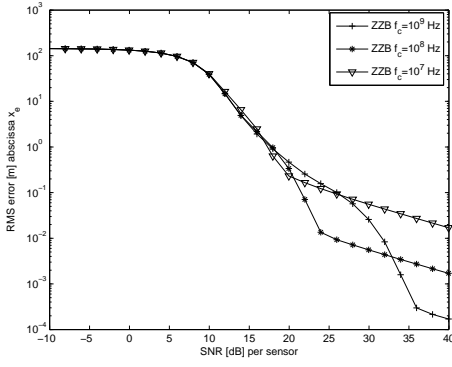


Figure 3.  $M = 8$ , transmitted bandwidth is  $B = 200$  kHz, and coordinates  $x_e$  and  $y_e$  are uniformly distributed on  $[-250$  m,  $250$  m]

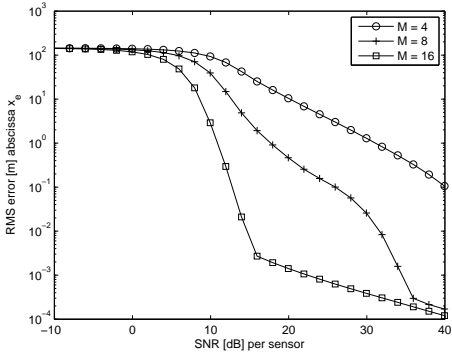


Figure 4.  $f_c = 1$  GHz, transmitted bandwidth is  $B = 200$  kHz, and coordinates  $x_e$  and  $y_e$  are uniformly distributed on  $[-250$  m,  $250$  m]

sidelobes with the carrier frequency. The effect of sidelobes in the localization metric can be reduced by increasing the number of sensors. This is illustrated in Fig. 4. The effect of bandwidth on localization is shown in Fig. 5. An increase in bandwidth causes a reduction in the sidelobes leading to smaller errors in the ambiguity region. This is due to the fact that the transmitted pulse autocorrelation function serves as the envelope of the localization metric. This envelope, which becomes narrower with the increase in bandwidth, forces the sidelobes to decay faster.

## V. CONCLUSION

The Ziv-Zakai bound for vector parameters was used to derive a lower bound on the MSE of estimating the location of a source. The bound provides a way to analyze localization performance at the full range of SNR values and parameterized by a quantities of interest such as carrier frequency, signal bandwidth, and number of sensors. Numerical examples demonstrate that the bound provides results close to the MLE over the whole frequency range. Three SNR regions are distinguishable for the bound. At low SNR, performance is dominated by noise, with false peaks popping up anywhere in the a priori parameter space of the source location. As the SNR increases, an transition region is observed, in which performance is dominated by the peak sidelobes of the localization metric. The performance at high SNR is ambiguity free, and the ZZB coincides with the CRLB.

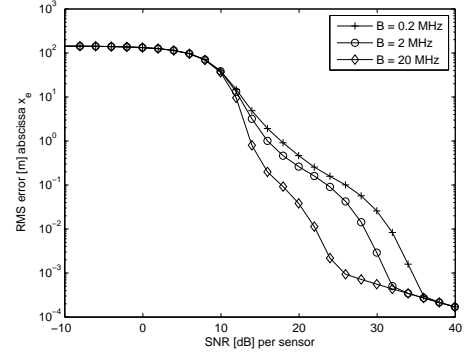


Figure 5.  $f_c = 1$  GHz, number of sensors is  $M = 8$ , and coordinates  $x_e$  and  $y_e$  are uniformly distributed on  $[-250$  m,  $250$  m]

## REFERENCES

- [1] N. Lehmann, A. Haimovich, R. Blum, and L. Cimini, "High resolution capabilities of MIMO radar," *40th Asilomar Conf. Signals, Systems and Computers*, pp. 25–30, Oct. 2006.
- [2] M. Haleem and A. Haimovich, "On the distribution of ambiguity levels in MIMO radar," *Asilomar Conf. Signals, Systems and Computers*, Oct. 2008.
- [3] S. Kay, *Fundamentals of Statistical Processing, Volume I: Estimation Theory*. Upper Saddle River, NJ: Prentice Hall PTR, 1993.
- [4] J. Ziv and M. Zakai, "Some lower bounds on signal parameter estimation," *IEEE Trans. Inf. Theory*, vol. 15, pp. 386–391, May 1969.
- [5] A. Weiss and E. Weinstein, "Fundamental limitations in passive time delay estimation - Part I: Narrow-band systems," *IEEE Trans. Acoust., Speech, Signal Process.*, vol. 31, pp. 472–486, Feb. 1983.
- [6] —, "Fundamental limitations in passive time delay estimation - Part II: Wide-band systems," *IEEE Trans. Acoust., Speech, Signal Process.*, vol. 32, pp. 1064–1078, Oct. 1984.
- [7] B. M. Sadler, L. Huang, and Z. Xu, "Ziv-Zakai time delay estimation bound for ultra-wideband signals," *IEEE International Conference on Acoustics, Speech, and Signal Processing*, vol. 3, pp. 549–552, Apr. 2007.
- [8] K. L. Bell, Y. Steinberg, Y. Ephraim, and H. L. V. Trees, "Extended Ziv-Zakai lower bound for vector parameter estimation," *IEEE Trans. Inf. Theory*, vol. 43, pp. 624–637, Mar. 1997.
- [9] K. L. Bell, Y. Ephraim, and H. L. V. Trees, "Explicit Ziv-Zakai lower bound for bearing estimation," *IEEE Trans. Signal Process.*, vol. 44, pp. 2810–2824, Nov. 1996.
- [10] A. Papoulis, *Probability Random Variables and Stochastic Processes*. McGraw Hill, 1991.
- [11] B. D. Steinberg, "The peak sidelobe of the phased array having randomly located elements," *IEEE Trans. on Antennas and Propagation*, vol. AP-20, pp. 129–136, March 1972.
- [12] H. L. V. Trees, *Detection, Estimation, and Modulation Theory, Part I*. New York: Wiley, 2001.
- [13] E. W. Barankin, "Locally best unbiased estimates," *Ann. Math. Stat.*, vol. 20, pp. 477–501, 1949.
- [14] D. Chazan, M. Zakai, and J. Ziv, "Improved lower bounds on signal parameter estimation," *IEEE Trans. Inf. Theory*, vol. 21, pp. 90–93, Jan. 1975.
- [15] A. J. Weiss, "Fundamental bounds in parameter estimation," Ph.D. dissertation, Tel-Aviv University, Tel-Aviv, Israel, 1985.
- [16] E. Weinstein and A. J. Weiss, "A general class of lower bounds in parameter estimation," *IEEE Trans. Inf. Theory*, vol. 34, pp. 338–342, Mar. 1988.
- [17] S. Bellini and G. Tartara, "Bounds on error in signal parameter estimation," *IEEE Trans. Commun.*, vol. 22, pp. 340–342, Mar. 1974.
- [18] L. D. Collins, "Asymptotic approximation to the error probability for detecting Gaussian signals," Cambridge, MA, 1968.
- [19] K. C. Ho and M. Sun, "Passive source localization using time differences of arrival and gain ratios of arrival," *IEEE Trans. Signal Process.*, vol. 56, pp. 464–477, Feb. 2008.
- [20] D. F. DeLong, "Use of the Weiss-Weinstein bound to compare the direction-finding performance of sparse arrays," MIT Lincoln Lab., Lexington, MA, Tech. Rep. Tech. Rep. 982, Aug. 1993.